ELSEVIER

Journal of Power Sources 77 (1999) 159–163

JOURNAL OF POWER SOURCES

Study of the performance of Ti–Zr based hydrogen storage alloys

H.J. Chuang, S.L.I. Chan *

Institute of Materials Science and Engineering, National Taiwan University, 1, Roosevelt Road, Sec. 4, Taipei 106, Taiwan

Received 8 October 1998; accepted 24 October 1998

Abstract

The P–C–I and charging–discharging properties of three Ti–Zr based alloys have been studied. Ni substitution for Mn and Cr in the alloy was found to increase the plateau pressure of the P–C–I curve. In addition, the partial substitution of Cr by V greatly improved the discharge capacity. However, the six-element alloy, $Ti_{0.5}Zr_{0.5}V_{0.2}Mn_{0.7}Cr_{0.5}Ni_{0.6}$, degraded rapidly in the gas–solid reaction. Hydrogen contents in the alloy under low pressure were increased during hydrogen absorption–desorption cycling. Annealing at 1050°C for 4 h before the P–C–I experiment helped in releasing the retained hydrogen under low pressure. Only a slightly flattened P–C–I slope was obtained for the annealed alloy. Microstructures of the as-cast and annealed alloys were examined and related to the above results. Alloy powder was poisoned after 2-month storage in air, which resulted in the deterioration of discharge capacity. Surface pretreatment on alloy powders by HCl–HF solution decreased the activation time of charge–discharge reaction.

Keywords: Hydrogen storage alloys; Degradation; Activation; P–C–I curves; Discharge capacity

1. Introduction

The nickel–metal hydride (Ni/MHx) battery employs a hydrogen storage alloy as the negative electrode material. It is used as a substitute for the Ni/Cd battery because of its high energy density, low pollution risk, absence of memory effect, stable voltage output and maintenance-free operation. The intensive research and development of hydrogen storage alloys further enhance the attraction of Ni/MHx batteries. Pressure–composition–isotherms represent the thermodynamic properties of metals in a gas-phase hydrogen environment, which does not necessarily correspond to the electrode reactions in an electrolyte. This is because of the difference in the kinetics of these two reactions, which have been discussed by Jerkiewicz and Zolfaghari [1]. The performance of metal hydrides as an electrode is highly related to the nature of hydrogen storage alloys. The composition of an alloy plays an important role in its properties, and much work has been devoted to this research [2–5]. It has been found by Jung et al. that vanadium is effective in increasing the electrical capacity [6]. Partially substituting Ni and Cr in the alloys by the elements V, Mn, etc. in the range 0.7–1.0 per AB_2 formula improves the hydrogen storage capacity and the electrochemical capacity of the alloy [7]. Fluoride and KOH pretreatment [8–12] are known to increase the activation rate. The oxide layer can be removed or damaged by fluorine pretreatment [11], which gives an active layer suitable for electrochemical reaction. The partial dissolution of some elements in an alloy in the electrolyte will also influence the electrochemical properties of the electrode. In a Zr–V–Ni system, the dissolution of V increases the electrode capacity [13]. The research by Liu and Suda [9], Liu et al. [10], and Sakashita et al. [11] showed that when the Zr–Ti–V–Ni alloy was treated with hot KOH solution, substantial corrosion and selective dissolution occurred because V and Zr were found to dissolve more than Ti and Ni. Thus the electrode was activated and a higher initial capacity compared with those without pretreatment was obtained.

AB_2 type hydrogen storage alloys composed of Ti–Zr–Mn–Cr were found to have a good hydrogen absorption and desorption [10], but then electrochemical capacity had not been investigated. In our previous work, a $Ti_{0.5}Zr_{0.5}Mn_1Cr_1$ alloy had been examined for hydrogen absorption–desorption by P–C–I and electrochemical measurements. The electrochemical capacity was poor. Substitutions of Cr and Mn by 0.6 atomic ratio of Ni did not improve its electrochemical capacity to a satisfactory level.

* Corresponding author. Fax: +886-2-23634562; E-mail: slichan@ccins.ntu.edu.tw

0378-7753/99/$19.00
PII: S0378-7753(98)00189-X

$Ti_{0.5}Zr_{0.5}V_{0.2}Mn_{0.7}Cr_{0.5}Ni_{0.6}$ was made by the addition of V to substitute part of Cr for the purpose of raising its capacity in the charge–discharge reaction. The thermodynamic and electrochemical behavior of $Ti_{0.5}Zr_{0.5}Mn_1Cr_1$, $Ti_{0.5}Zr_{0.5}Mn_{0.7}Cr_{0.7}Ni_{0.6}$ and $Ti_{0.5}Zr_{0.5}V_{0.2}Mn_{0.7}Cr_{0.5}Ni_{0.6}$ alloys have been compared based on their P–C–I curves and discharge capacities. Preliminary work on the fluoride acid pretreatment has also been carried out.

2. Experimental details

Three Ti–Zr–Mn–Cr based alloys, $Ti_{0.5}Zr_{0.5}Mn_1Cr_1$ (code G), $Ti_{0.5}Zr_{0.5}Mn_{0.7}Cr_{0.7}Ni_{0.6}$ (code K) and $Ti_{0.5}Zr_{0.5}V_{0.2}Mn_{0.7}Cr_{0.5}Ni_{0.6}$ (code L) were prepared by non-consumable (W) electrode arc melting under a reduced pressure argon atmosphere on a water-cooled copper hearth. The ingots were remelted eight times to ensure homogeneity throughout the ingot. Raw materials used were Zr, V, Cr, Ni pellets, Ti rod and electrolytic Mn. All starting materials were at least of a purity $>99.7\%$. The as-cast alloy was crushed and ground mechanically, then sieved. Part of the ingot was annealed for 4 h at 1050°C. A half-automated Sievert's type apparatus was developed to measure the hydrogen absorption–desorption reaction of the alloy at room temperature. The P–C–I experiments were performed and carried out directly on the ingot and pulverization was achieved during absorption–desorption cycling.

Crystal structure was identified by X-ray diffraction patterns using continuous scan mode. Surface morphology was studied by employing SEM. To identify the composition of the alloys, EDS and EPMA were used. Surface treatment was performed by stirring the alloy powders in a 0.02N HCl solution for 30 min, followed by stirring in 0.014 N HF solution for 5 h at room temperature.

An alloy electrode was prepared by the pasting method. The alloy powders (<65 μm) were mixed thoroughly with Ni powder (IN-255) in a ratio of 1:3. PTFE (3%) was added as a binder. The above mixture was pasted onto a piece of nickel mesh, then pressed at 2 tons/cm^2 for 1 min. The charge–discharge performance was measured in a test cell composed of alloy electrode as the anode and $Ni(OH)_2$ as the cathode. Polypropylene was used as the separator between the cathode and the anode. Electrolyte solution consisted of 30 wt.% KOH + 1 wt.% LiOH. The cell was anodically limited at a charge rate of 20 mA/g, and discharged at the same rate to 1.0 V.

3. Results and discussion

3.1. The pressure–composition–isotherm curves

The P–C–I curves of three alloys studied in this work are shown in Fig. 1. At 25°, $Ti_{0.5}Zr_{0.5}Mn_1Cr_1$ alloy had a

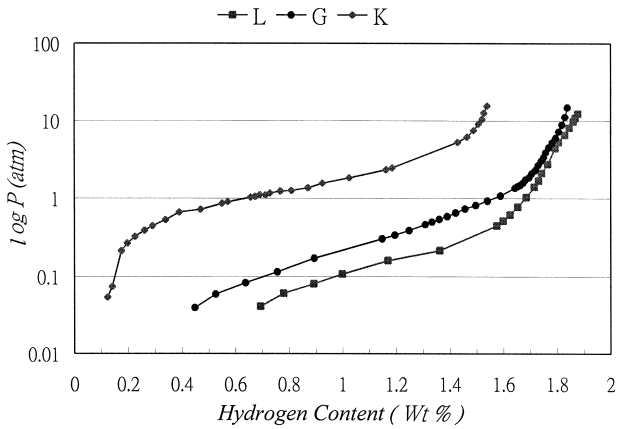

Fig. 1. Pressure–composition–isotherm curves of the alloys studied at 25°C. G: $Ti_{0.5}Zr_{0.5}Mn_1Cr_1$; K: $Ti_{0.5}Zr_{0.5}Mn_{0.7}Cr_{0.7}Ni_{0.6}$; L: $Ti_{0.5}Zr_{0.5}V_{0.2}Mn_{0.7}Cr_{0.5}Ni_{0.6}$.

hydrogen storage capacity of 1.8 wt.% under 10 atm equilibrium pressure and 0.45 wt.% under 0.04 atm. When alloying with 0.6 atomic ratio Ni to substitute Cr and Mn, the plateau pressure of P–C–I curve of $Ti_{0.5}Zr_{0.5}Mn_{0.7}Cr_{0.7}Ni_{0.6}$ (specimen K) was obviously increased, which is consistent with the results presented by Liu et al. [10]. However, its slope was not affected. The amount of hydrogen retained in the alloy under 0.04 atm equilibrium pressure decreased, which may indicate an improvement in the reversibility of the hydrogen absorption–desorption reactions. It has been suggested that the increase of Ni content reduced its cell volume, and increased its plateau pressure in hydrogen absorption–desorption reaction [10]. When V was added to substitute part of Cr in the alloy, the plateau pressure was the lowest among these three alloys. The hydrogen storage capacity of the $Ti_{0.5}Zr_{0.5}V_{0.2}Mn_{0.7}Cr_{0.5}Ni_{0.6}$ alloy increased a little compared with of the four-element alloy under high pressure, but there was up to 0.6 wt.% of hydrogen under low pressure that cannot be released at room temperature. A steeper slope in the plateau area of this alloy implies that more phases than that in the five-element alloy may be formed by the substitution of V.

The desorption curves of $Ti_{0.5}Zr_{0.5}V_{0.2}Mn_{0.7}Cr_{0.5}Ni_{0.6}$ shown in Fig. 2 indicate a high degradation rate during cycling. The retained hydrogen in the specimen under 0.04 atm hydrogen environment after the 2nd cycle was 0.8 wt.%, and that after the 3rd cycle was up to 1 wt.%, while that after the 1st cycle was only 0.6 wt.%. This behavior may come from phase transformations and pulverization of alloy in the absorption–desorption reaction. The variation of slope in the plateau area suggests that new phases were formed during the hydrogenation reaction, which is irreversible. Also, the formation of microcracks during desorption process created fresh surfaces. These fresh surfaces absorbed part of the released hydrogen in the desorption step, which gave rise to the increase in retained hydrogen in the alloy. If the diffusion rate of hydrogen in the hydride

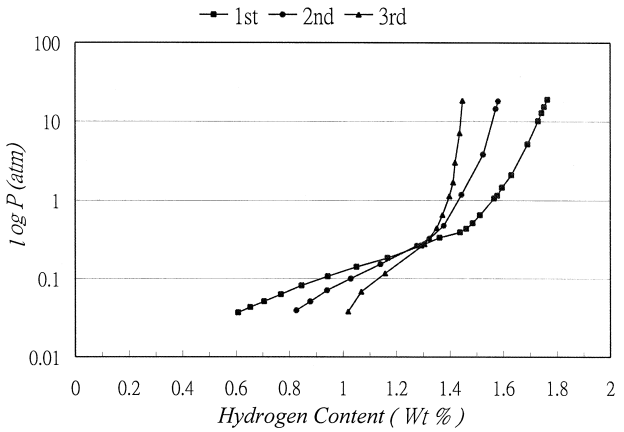

Fig. 2. The desorption curves of $Ti_{0.5}Zr_{0.5}V_{0.2}Mn_{0.7}Cr_{0.5}Ni_{0.6}$ alloy for the first three cycles.

is slower than that in the bare alloy, the newly formed hydride layer would act as a barrier for further hydrogen absorption. This pulverization mechanism thus provides an explanation for the irreversibility of this alloy.

We have performed an experiment on the rate of hydrogen breakthrough in the ingot, and it was found that the absorption rate of the annealed ingot was obviously delayed. It took 75 s for hydrogen to break through the as-cast alloy, while it took 92 min to break through the annealed alloy. Surface oxidation is one of the reasons, and phase transformation may also give contribution. When desorption curves of as-cast and annealed specimens are compared (Fig. 3), a decreasing hydrogen capacity of the annealed specimen under high pressure is shown. However, less hydrogen was retained in the annealed alloy under 0.04 atm. The slopes of those curves show that multiphases coexisted in the as-cast and annealed alloy. A similar result was reported by Liu et al. [10]. It was possible that a 4-h annealing was not long enough to eliminate segregation. But the slope of the annealed alloy is flattened a little in the low-pressure region. Since the alloy is composed of different phases, only some of the phases had good hydrogen absorption. From the micro-

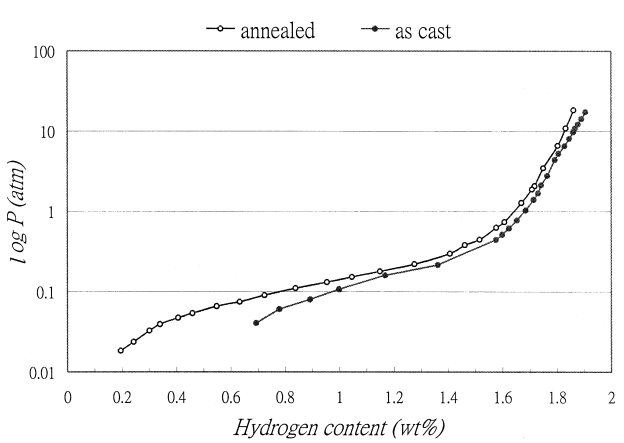

Fig. 3. The desorption curves of annealed and as-cast alloys.

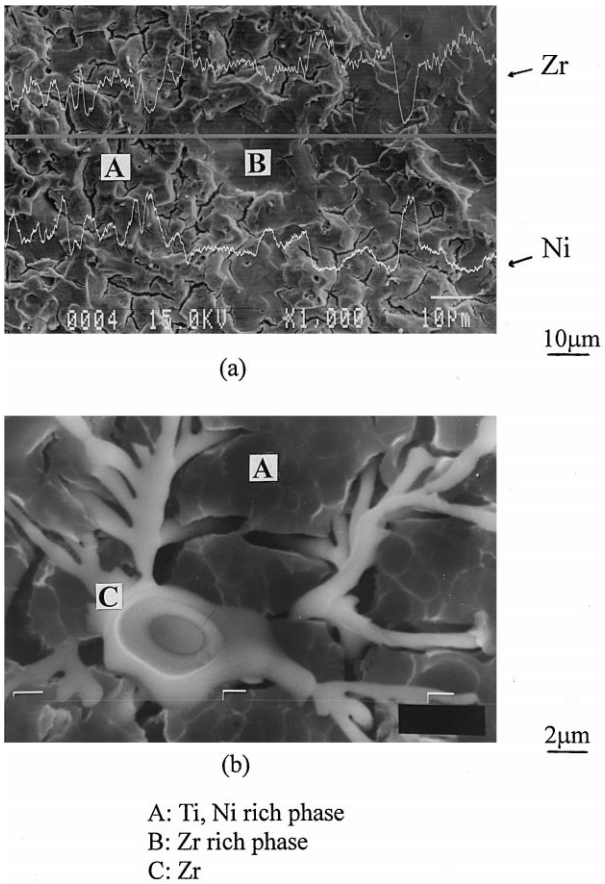

Fig. 4. Surface morphology of the as-cast alloy. (a) EPMA line scan of Zr and Ni; (b) Pure Zr existence in the ingot.

graphs and the EPMA line scan of the as-cast alloy, there were some pure Zr particles found in the as-cast ingot (Fig. 4), which disappeared after 4-h annealing. Other than the pure Zr particles, there were at least two main phases found in the as-cast alloy. The one with a lot of cracks was found to be a Ti–Ni rich phase, while the other one was a Zr-rich phase. The annealed alloy was also composed of two main phases, one Zr-rich and one Ti-rich, which had been found by our work on EDS and EPMA analysis. It is believed that the new phases formed in the annealing process absorbed less hydrogen than the old phases, but desorbed more under low pressure. Further studies are underway to investigate their individual performance. The effect of annealing for a longer time will also be studied in future work.

3.2. The electrochemical properties

Although the three alloys studied here, namely $Ti_{0.5}Zr_{0.5}Mn_1Cr_1$, $Ti_{0.5}Zr_{0.5}Mn_{0.7}Cr_{0.7}Ni_{0.6}$ and $Ti_{0.5}Zr_{0.5}V_{0.2}Mn_{0.7}Cr_{0.5}Ni_{0.6}$, all possessed reasonably good hydrogen capacity in the gas–solid reaction, the electrochemical capacity was found to be poor for the first two alloys (Fig. 5). The discharge capacity was obviously

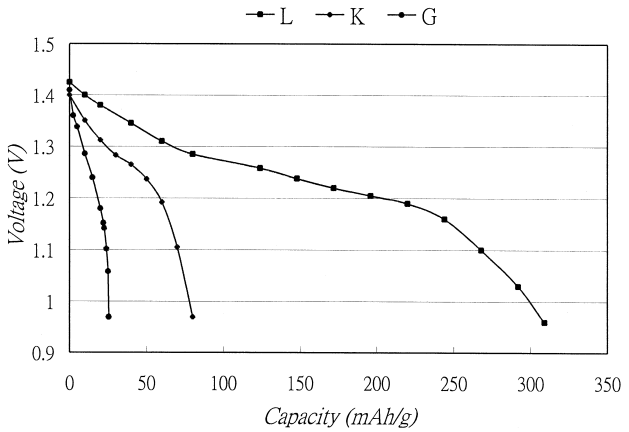

Fig. 5. Specific discharge capacity of the alloys studied. G: $Ti_{0.5}Zr_{0.5}Mn_1Cr_1$; K: $Ti_{0.5}Zr_{0.5}Mn_{0.7}Cr_{0.7}Ni_{0.6}$; L: $Ti_{0.5}Zr_{0.5}V_{0.2}Mn_{0.7}Cr_{0.5}Ni_{0.6}$.

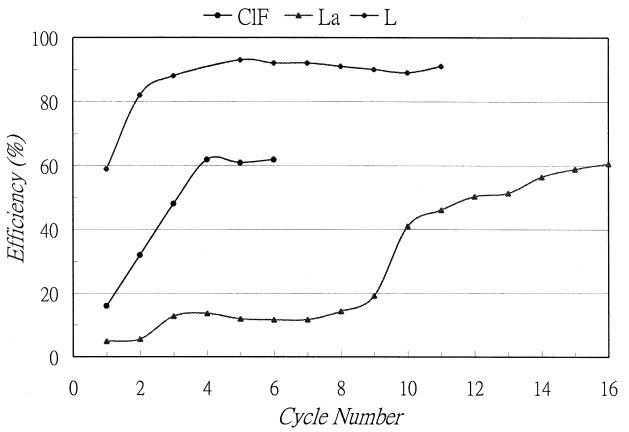

Fig. 6. Activation performance of $Ti_{0.5}Zr_{0.5}V_{0.2}Mn_{0.7}Cr_{0.5}Ni_{0.6}$. ClF: alloy powders were treated with HCl–HF solution; La: alloy powders were annealed at 1050°C for 4 h; L: as-cast alloy powder without any treatment.

increased by the substitution of V (the L alloy in Fig. 5). The large improvement may be attributed to the leaching of V (Table 1) from alloy electrode immersed in the electrolyte before and during charge–discharge cycling. It had been suggested by Jung et al. [14] that a Ni-rich phase is created on the electrode surface and this provides active sites for the reaction. It is also possible that the increment in discharge capacity might result from catalytic effects during charge–discharge reactions by the dissolved V in the electrolyte solution.

Remarkable deterioration was found on the capacity of the alloy powders stored under air at room temperature. The powders freshly pulverized by hydriding–dehydriding cycling have a capacity of 300 mA h/g. Half of their capacity was lost after 2-month storage in air. The discharge efficiencies of $Ti_{0.5}Zr_{0.5}V_{0.2}Mn_{0.7}Cr_{0.5}Ni_{0.6}$ in Fig. 6 show that annealing decreases the discharge capacity and the activity of the alloy. Discharge efficiency of the freshly prepared alloy was over 90% and fully activated in five cycles, while that of the annealed alloy was around 10% in the first five cycles, and rose to 60% after the 16th cycle. This phenomenon may have resulted from the surface poisoning by O_2, H_2O, ... in the air. It is suggested that a large change during the 10th cycle of the annealed alloy was due to the breakthrough of the poisoned layer on the powder surface. The effect of surface treatment on these poisoned powders by HCl–HF solution can be observed in Fig. 6. The activation rate as expressed by discharge efficiency was increased to 60% at the 4th cycle. However, that was still lower than the freshly prepared powders. Based on the preliminary study of fluorination of this AB_2 material, it was found to have a positive influence on the poisoned alloy. However, there is room for improvement of the fluorination procedure to restore this poisoned alloy to an activated state.

Table 1
The concentration of dissolved elements after immersion in electrolyte solution for 2 weeks (in ppm)

Alloy	Ti	Zr	V	Mn	Cr
L	2.5	44.4	154	3.1	4.6
G	6.2	56.9	–	7.4	60.6
K	2.83	22.6	–	3.4	10.7

4. Conclusion

$Ti_{0.5}Zr_{0.5}V_{0.2}Mn_{0.7}Cr_{0.5}Ni_{0.6}$ is a multiphase alloy with a plateau pressure below 1 atm. Hydrogen content in the gas–solid reaction for the first cycle was around 1.8 wt.%, but decreased during the absorption–desorption cycling. This rapid degradation was attributed to the pulverization of alloy. Annealing at 1050°C for 4 h helped release the absorbed hydrogen under low pressure, but had little influence both on the total capacity at high pressure and the slope of plateau pressure. Discharge capacity was improved significantly to 300 mA h/g, which was 200 mA h/g more than $Ti_{0.5}Zr_{0.5}Mn_{0.7}Cr_{0.7}Ni_{0.6}$ and much more than $Ti_{0.5}Zr_{0.5}Mn_1Cr_1$.

V substitution plays an important role in electrochemical reactions. These results indicate that the hydrogen absorption–desorption behavior in gas–solid interaction does not correspond to that in the charging–discharging reactions. Storage of the alloy powders under air for 2 months reduced the discharge capacity significantly. The activation time of charge–discharge reaction has been reduced by HCl–HF surface treatment on the poisoned alloy powders.

Acknowledgements

The authors are grateful for the supply of the alloys from Chung-Sang Institute of Science and Technology, Lung-Tan, Taoyuan, Taiwan.

References

[1] G. Jerkiewicz, A. Zolfaghari, J. Electrochem. Soc. 143 (4) (1996) 1240.
[2] C. Iwakura, T. Oura, H. Inoue, M. Masao, Electrochim. Acta 41 (1996) 117.
[3] B. Luan, N. Cui, H.K. Liu, H.J. Zhao, S.X. Do, J. Power Sources 55 (1995) 197.
[4] K. Petrov, A.A. Rostami, A. Visintin, S. Srinivasan, J. Electrochem. Soc. 141 (1994) 1747.
[5] M. KopcZyk, G. Wojcik, G. Mlynarek, A. Sierczynska, M. Beltowska-Brzezinska, J. Appl. Electrochem. 26 (1996) 639.
[6] J.H. Jung, K.Y. Lee, J.Y. Lee, J. Alloys Compounds 226 (1995) 166.
[7] X.G. Yang, Y.Q. Lei, W.K. Zhang, G.M. Zhu, Q.D. Wang, J. Alloys Compounds 243 (1996) 151.
[8] H.H. Uchida, Y. Watanabe, Y. Matsumura, H. Uchida, J. Alloys Compounds 231 (1995) 679.
[9] F.J. Liu, S. Suda, J. Alloys Compounds 230 (1995) 58.
[10] F.J. Liu, S. Suda, G. Sandrock, J. Alloys Compounds 232 (1996) 232.
[11] M. Sakashita, Z.P. Li, S. Suda, J. Alloys Compounds 253–254 (1997) 500.
[12] D. Chartouni, A. Zuttle, C. Nutzenadel, L. Schlapbach, J. Alloys Compounds 260 (1997) 265.
[13] X.P. Gao, W. Zhang, H.B. Yang, D.Y. Song, Y.S. Zhang, Z.X. Zhou, P.W. Shen, J. Alloys Compounds 235 (1996) 225.
[14] J.H. Jung, B.H. Liu, J.Y. Lee, J. Alloys Compounds 264 (1998) 306.